Chandra Observations of Supersonic Pulsar Wind Nebulae

THE GEORGE WASHINGTON UNIVERSITY
WASHINGTON, DC

Oleg Kargaltsev (George Washington University), Noel Klingler (PSU), George Pavlov (PSU),
Bettina Posselt (University of Oxford / PSU), Roger Romani (Stanford University), Patrick Slane (Harvard University)

CXO observations have revolutionized studies of pulsar wind nebulae (PWNe). In particular, they have led to the discovery of X-ray emission from pulsar tails. These extended structures are ram-pressure confined regions behind supersonically moving pulsars filled with ultra-relativistic pulsar wind. CXO data on pulsar tails fueled theoretical and computational studies which include mass entrainment, turbulence, reconnection, kinetic particle escape, and MHD modeling. We present the results from recent observing campaigns where several supersonic PWNe (SPWNe) have been observed with deep CXO exposures. Using ACIS to perform spatially resolved spectroscopy, we found that some tails exhibit strong spectral softening along their lengths (consistent with rapid cooling) while others do not. The absence of cooling may require particle re-acceleration (e.g., via magnetic turbulence and reconnection). The unprecedented angular resolution of CXO also revealed distorted structures of compact nebulae associated with long pulsar tails, which allows one to study the connection between the properties of both compact and extended components and with the gamma-ray and radio light curves of the pulsars. Finally, deep ACIS images of several SPWNe revealed completely unexpected structures dubbed ``misaligned outflows" (a.k.a. kinetic jets) that can extend for several parsecs at large angles with respect to the pulsar velocity, have hard spectra, and exhibit puzzling morphologies.

Supersonic Pulsar Wind Nebulae

Effects of pulsar velocity on its nebula

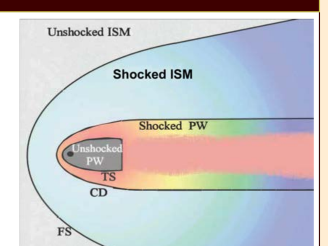

- If pulsar's velocity, v_{psr}, exceeds the sound speed, c_s, in the ambient medium its PWN is strongly affected by the ram pressure;
- **Subsonic PWNe,** $\mathcal{M} = \frac{v_{psr}}{c_s} \ll 1$; Examples: Crab PWN
- **Supersonic PWNe (SPWNe),** $\mathcal{M} = \frac{v_{psr}}{c_s} \gg 1$; Examples: Mouse PWN
- **Transonic PWNe (TPWNe),** $\mathcal{M} = \frac{v_{psr}}{c_s} \sim 1$; Examples: Vela PWN, PWN of PSR B1706-44 (see poster by Martijn DeVries)
- Subsonic PWNe often (when resolved well) exhibit torus-jet morphologies; their pulsars can be moving fast but $\mathcal{M} = \frac{v_{psr}}{c_s} \ll 1$ because of the large c_s (for instance in the young SNR interior where the temperature is high)

$c_s = (\gamma_{\rm ad} kT/\mu m_{\rm H})^{1/2} \sim 3\text{–}30\ {\rm km\ s^{-1}}$ a reasonable estimate for ISM sound speed

$p_{\rm ram} = \rho_{\rm amb} V_{\rm psr}^2 = 1.5\times10^{-9} n_b (V_{\rm psr}/300\,{\rm km\,s^{-1}})^2\ {\rm dyn\ cm^{-2}}$ where n_b is the baryon number density and $p_{\rm ram}/p_{\rm amb} = \gamma_{\rm ad}\mathcal{M}^2$

Properties of supersonic pulsar wind nebulae (SPNWe)

- A characteristic (stand-off) distance, R_0, at which the ram pressure of the pulsar wind balances the ram pressure:

$$R_0 = \left(\frac{\dot E_w}{4\pi c p_{\rm ram}}\right)^{1/2} = 1.3\times10^{16} \dot E_{w,35}^{1/2} n_b^{-1/2} (V_{\rm psr}/300\,{\rm km\,s^{-1}})^{-1}\ {\rm cm}$$

- The corresponding stand-off angular scale is difficult to resolve even with CXO:

$$\theta_0 \approx R_0/d = 0.''89 d_{1.0}^{-1} \dot E_{w,35}^{1/2} n_b^{-1/2} (V_\perp/300\,{\rm km\,s^{-1}})^{-1} \sin i.$$

- Magnetic field inside the PWN near the stagnation point (i.e. at $r \approx R_0$):

$$B \sim \left[\frac{\dot E_w \sigma}{c R_0^2(\sigma+1)}\right]^{1/2} = \left(\frac{4\pi p_{\rm ram}\sigma}{\sigma+1}\right)^{1/2} \approx 140 \left(\frac{n_b\sigma}{\sigma+1}\right)^{1/2} \frac{V_{\rm psr}}{300\,{\rm km\,s^{-1}}}\ \mu{\rm G}$$

should be about 10-100 μG for reasonable values of magnetization $\sigma \le 1$.

- Typical energies of synchrotron photons emitted in such fields can be estimated as

$$E = \zeta \frac{heB_\perp \gamma^2}{2\pi m_e c} = 1.16 \zeta B_{-5} \gamma_8^2\ {\rm keV}$$

where E_e are the electron energies, $\zeta \sim 1$;

- The maximum Lorentz factor of accelerated electrons: $\gamma_{\rm max} \lesssim (e/m_e c^2)[\dot E\sigma/c(\sigma+1)]^{1/2} \approx 1.1\times10^9 \dot E_{35}^{1/2} [\sigma/(\sigma+1)]^{1/2}$ follows from requiring the electron Larmor radius $R_g < R_0$, where $R_g = \gamma m_e c^2/(eB) = 1.7\times10^{16} \gamma_8 B_{-5}^{-1}\ {\rm cm}$
- This limits synchrotron photon energies to $E_{\rm max} \lesssim 130 \zeta \dot E_{35} B_{-5} \sigma/(\sigma+1)$ keV suggesting that old or low-$\dot E$ pulsars or those with low magnetization should not be sources of synchrotron emission in X-rays.
- SPWNe around all pulsars can still be visible in radio, optical/near-IR (including H_α from shocked ISM) and far-UV.

Recent numerical modeling of SPWNe: toward a realistic picture

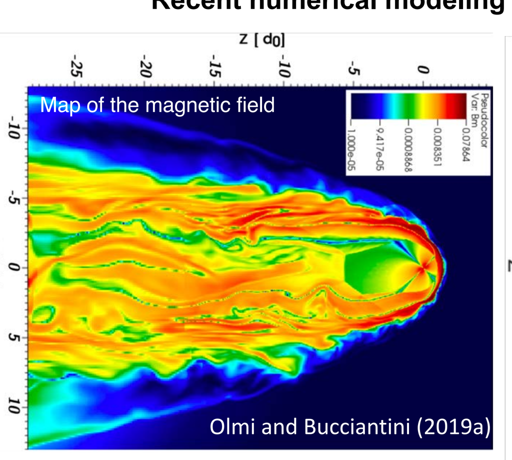

Full 3D RMHD with anisotropic wind ejection.

Jets are not discernible at large distances in and do not seem to bend with the distance from the pulsar as suggested by CXO images.

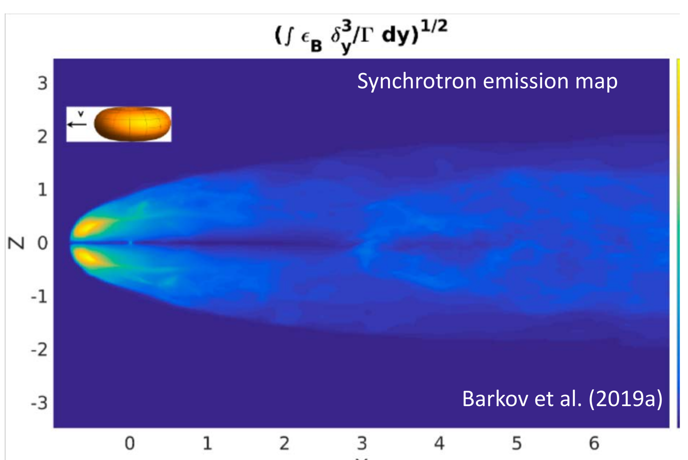

3D RMHD simulations of the interaction of magnetized pulsar wind with magnetized external medium.

Structures looking like jets deformed by the motion can be seen up to substantial distances from the pulsar.

Pulsar velocities (supernova kicks)

- **Transverse velocity and parallax measurements (mostly in radio) exist for ~160 pulsars (Jankowski et al. 2019; Deller et al. 2019).**

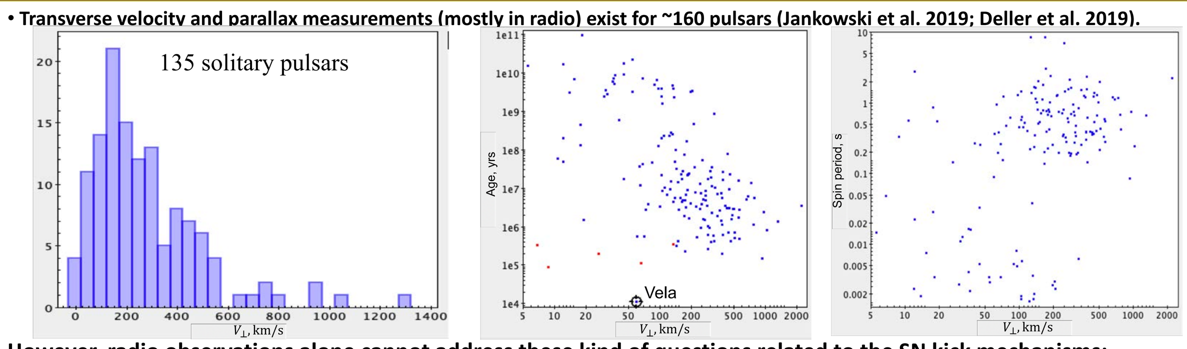

However, radio observations alone cannot address these kind of questions related to the SN kick mechanisms:

- Are there pulsars kicked strongly along their spin axis?
- Are there strongly kicked pulsars with aligned spin-magnetic axis?

By observing PWNe with CXO one can determine the positional angle of rotation axis and, with some theoretical modeling involving the gamma-ray and radio lightcurves, the angle between the spin and magnetic dipole axis. This allows one to tackle the above questions once $V_\perp$ is measured in radio. The presence of the host SNR or nearby massive open clusters projected in the pulsar vicinity (with distances provided by Gaia) provide constraints on the distance to the pulsar when the radio parallax is not available. At the moment the PWN structures show that a strong kick can be imparted onto a NS in the direction perpendicular to its spin axis. There is no solid evidence for the spin-aligned **strong** kicks. *Deeper CXO observations of other SPWNe can help to find such cases or establish their absence.*

- **Teaser question**: Is there a deceleration force acting on the a pulsar surrounded by a SPWN ? The role of entrainment from ISM affecting the shocked pulsar wind flow has been discussed in Morlino et al. (2015) & Olmi (2018).

SPWNe of millisecond pulsars

- **Extended emission seen around few recycled (millisecond) pulsars is consistent with SPWN interpretation (e.g., H_α bowshocks).**
- **In X-rays SPWNe of millisecond pulsars show diverse structures. This diversity is not yet understood.**

SPWN of PSR J2124–3358

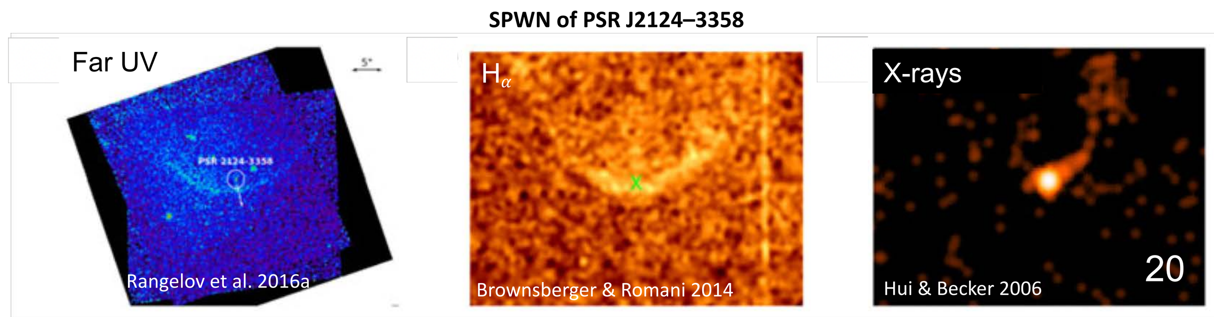

SPWN of PSR J0437-4715

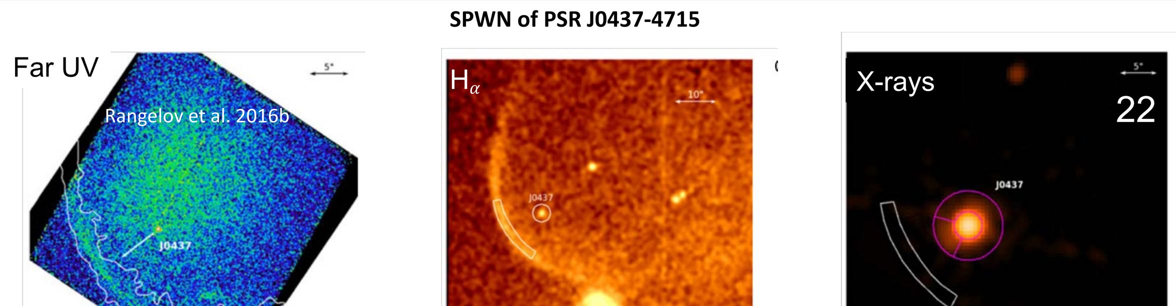

SPWN of black widow PSR B1957+20:
(X-rays – red; H_α – green)

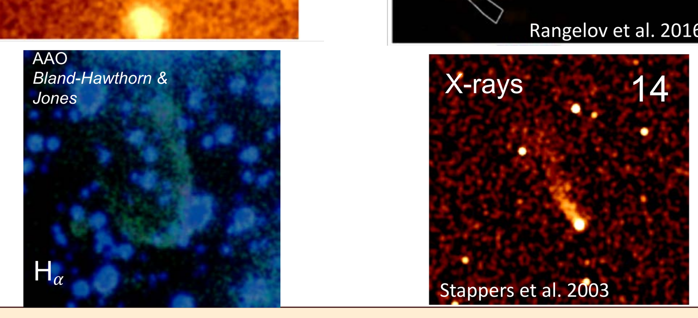

Recent observations of PSR J1016-5857

The shape of X-ray PWN indicates a low-to-modest $\mathcal{M}$.

The radio nebula morphology is puzzling, it does not resemble other pulsar tails.

Analysis is ongoing.

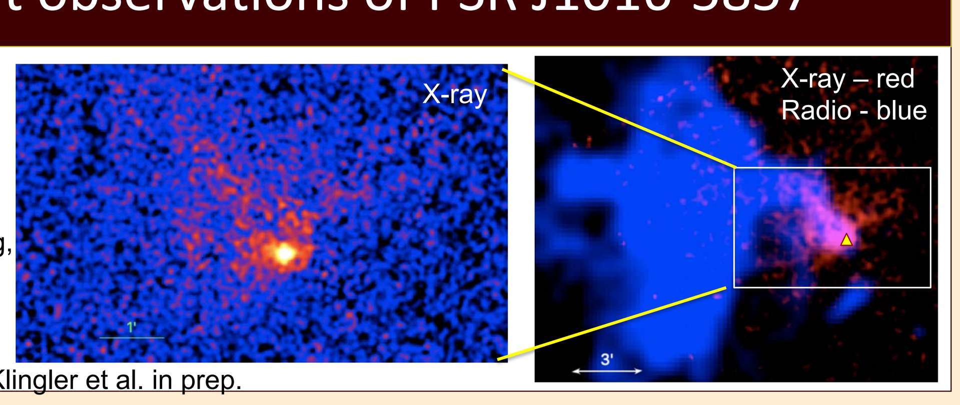

Klingler et al. in prep.

Current sample of SPWNe

- **SPWNe and TPWNe constitute about 30% of known PWN population**
- **SPWNe are detected in radio, H_α, X-rays, but not in GeV or TeV gamma-rays**
- **In the table below SPWNe are highlighted, the rest are TPWNe**

See review by Kargaltsev et al. (2017) and references therein.

#	Pulsar	Associated object(s)	d (kpc)	$\log \dot E$ (erg s^{-1})	$\log \tau$ yrs	B_{11} (10^{11} G)	$v_\perp$ (km s^{-1})	i (deg.)	l (pc)	$\log L_X$ (erg s^{-1})	$\log \eta_X$	$H\alpha$	Rad.
1	J0537–6910[a]	N157B	49.7	38.68	3.69	9.25	—	—	3.7	36.21 ± 0.01	−2.47	N	N
2	B1951+32	CTB 80	3	36.57	5.03	4.86	460	—	1.2	33.02 ± 0.11	−3.55	?[a]	Y[a]
3	J1826–1256	HESS J1825–137	~3.9[c]	36.56	4.16	37	—	—	5.8	33.38 ± 0.06	−3.18	?	?
4	B1706-44	G343.1–2.3	2.6	36.53	4.24	31.2	$\lesssim$100	?	3	32.60 ± 0.10	−3.93	N	Y
5	B1757–24	G5.27–0.9, Duck PWN	3.8	36.41	4.19	40.4	198	—	0.4	33.20 ± 0.14	−3.21	?	Y
6	J1747–2958	Mouse PWN	5	36.40	4.41	24.9	306 ± 43	~20°	1.1	33.83 ± 0.09	−2.57	?	Y
7	J1135–6055	—	~2.8[c]	36.32	4.36	30.5	<330	—	1.4	32.40 ± 0.04	−3.92	?	?
8	J1437–5959	G315.9–0.0, Frying Pan PWN	8	36.15	5.06	7.37	~300	—	~20	—	—	?	Y
9	J1101–6101	G290.1–0.8, Lighthouse PWN	~7[c]	36.13	5.06	7.24	~2000	—	3.5	32.40 ± 0.40	−3.31	?	Y
10	J1509–5850	—	4	35.71	5.19	9.14	200–600	~90°	6.5	33.05 ± 0.04	−2.66	Y	Y
11	B0906–49	—	1	35.69	5.05	12.9	~60	~90°	3.5	—	−5.86	?	Y
12	B1853+01[a]	W44	3.3	35.63	4.31	75.5	400^{+114}_{-73}	—	1.3	32.20 ± 0.10	−2.58	N	N
13	B0740–28	—	2	35.28	5.2	16.9	275[d]	—	—	—	—	Y	?
14	B1957+20	the Black Widow pulsar	1.73	35.20	9.18	0.002	~220	—	0.3	29.73 ± 0.40	−5.14	Y	?
15	J0538+2817	S147	1.39[b]	34.69	5.79	7.33	357^{+59}_{-43}	~90°	0.02	31.30 ± 0.15	−3.39	N	N
16	B0355+54	Mushroom PWN	1.04[b]	34.66	5.75	8.39	61^{+12}_{-9}	<20°	1.5	31.20 ± 0.07	−3.46	?	N
17	J0633+1746	Geminga PWN	0.25[b]	34.51	5.53	16.3	~200	> 50°	0.35	29.35 ± 0.11	−5.53	?	?
18	J2030+4415	—	~1[c]	34.46	5.74	12.3	—	—	0.07	30.49 ± 0.18	−3.97	Y	N
19	J1741–2054	—	0.3	33.97	5.59	26.8	155	~75°	0.5	30.21 ± 0.02	−3.76	Y	?
20	J2124–3358	—	0.41	33.83	9.58	0.003	75[d]	—	0.04	28.98 ± 0.15	−4.85	Y	Y
21	J0357+3205	Morla PWN	0.5	33.77	5.73	24.3	~2000	> 70°	1.3	30.07 ± 0.20	−3.70	N	N
22	J0437–4715	—	0.156[b]	33.74	9.2	0.006	104.7 ± 0.9	~58°	—	~28.6	−6.2	Y	?
23	J2055+2539[a]	—	~0.6[c]	33.69	6.09	11.6	$\lesssim$2300	—	~1.7	30.17 ± 0.03	−3.53	?	?
24	B1929+10	—	0.36[b]	33.59	6.49	5.18	177^{+4}_{-5}	~60°	1.5	29.50 ± 0.25	−4.09	?	Y
25	B2224+65	Guitar Nebula	1.88	33.07	6.05	26	1626	—	0.6	30.18 ± 0.10	−2.89	Y	N
26	—	IC443[a]	1.4	—	—	—	~250	—	0.65	32.82 ± 0.03	—	N	Y
27	—	MSH 15–56, G326.3–1.8	4	—	—	—	100–400	—	3.5	32.8 ± 0.2	—	?	Y
28	—	G327.1–1.1, Snail PWN	7	—	—	—	~500	—	5.6	33.09 ± 0.10	—	?	Y

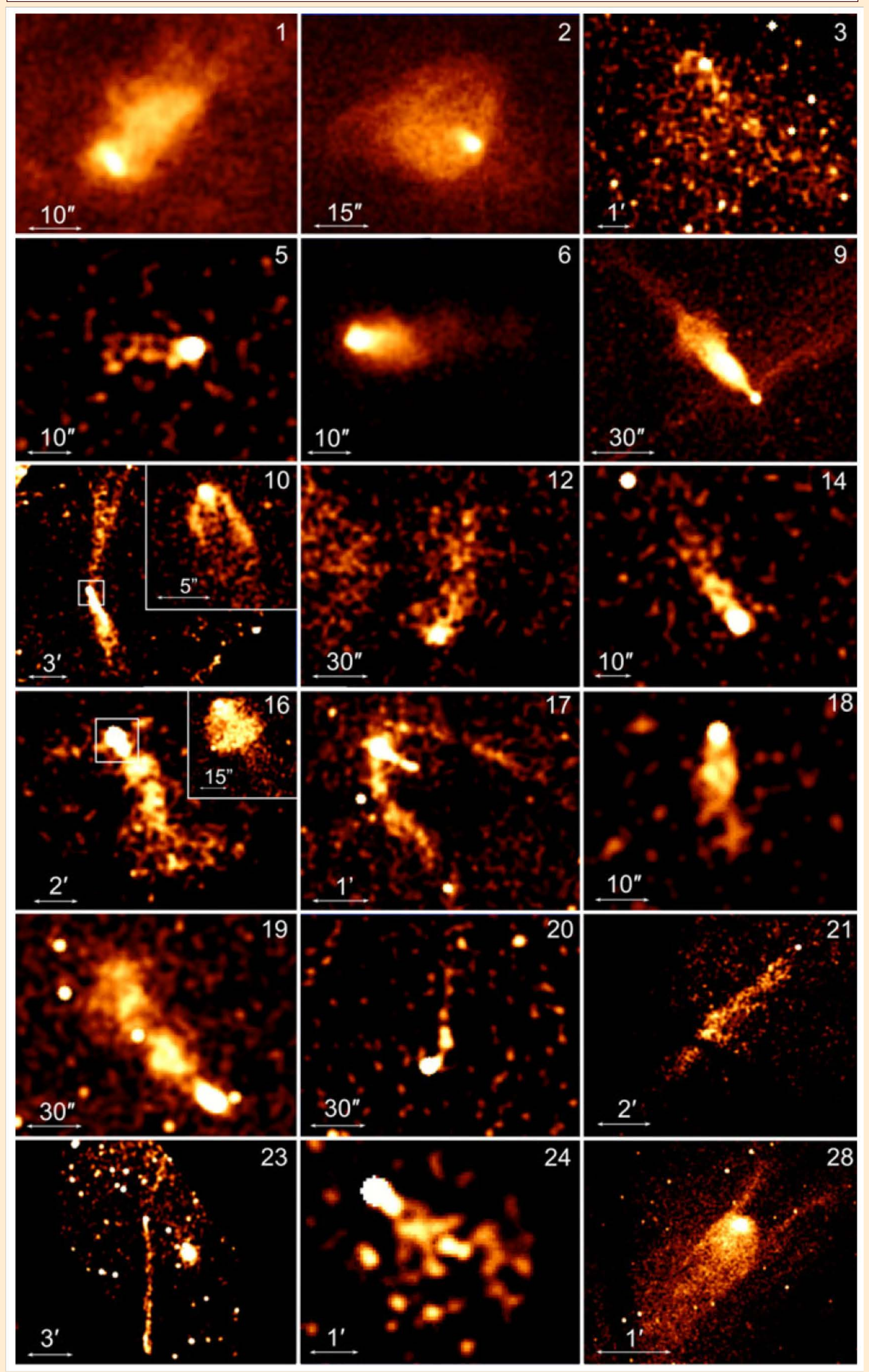

SPWN-SNR connection

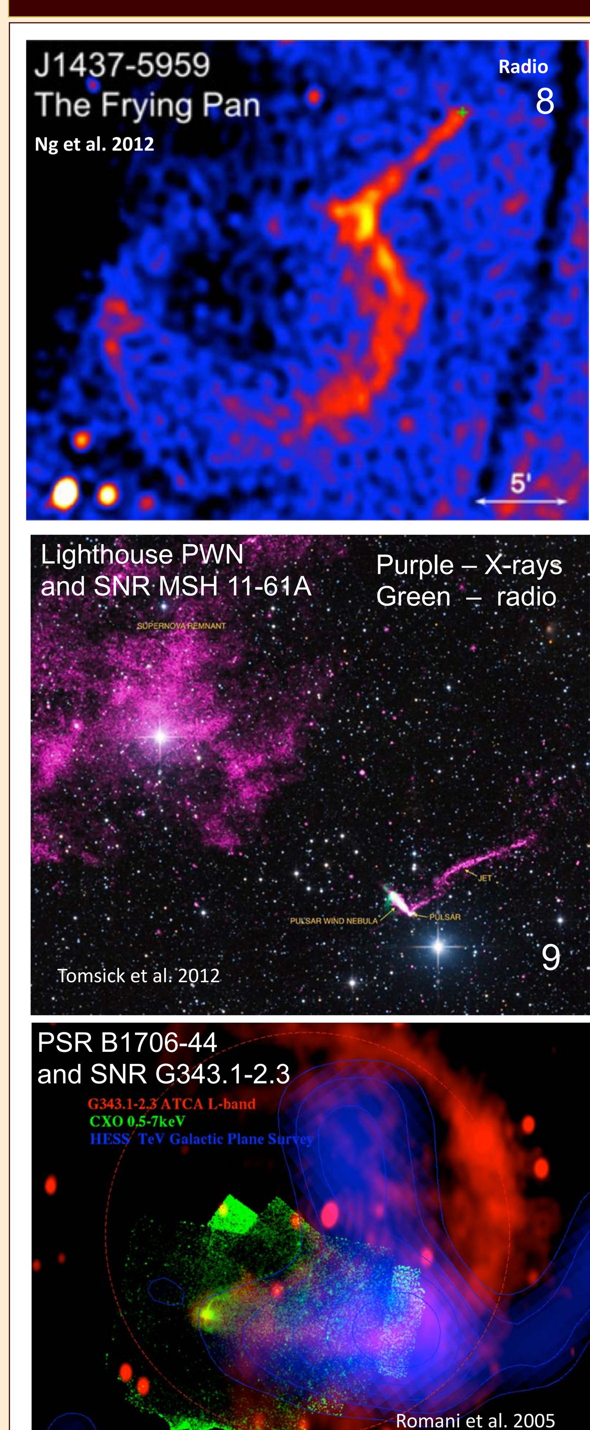

See also poster by Marttijn De Vries !

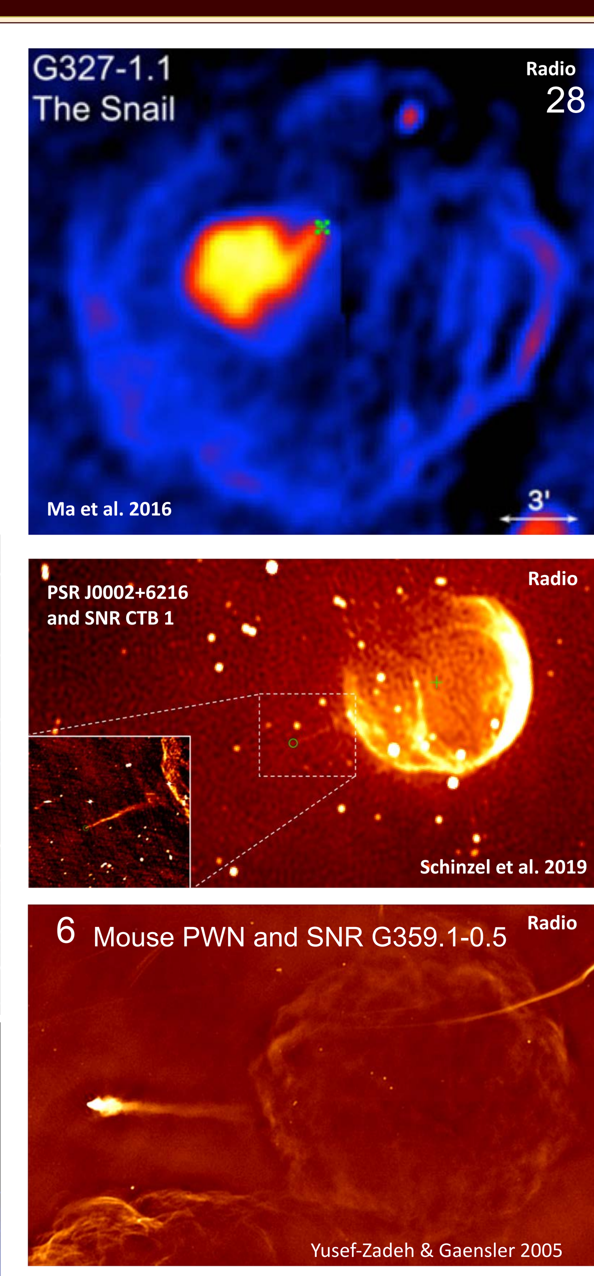

About 10 pulsars with SPWNe (or TPWNe) have credible evidence of association with a nearby SNR. It is imperative to measure their proper motions and parallaxes in radio, if feasible.

Torus-jet structures of SPWNe heads

- **Three principal geometries from Barkov et al. (2019a):**

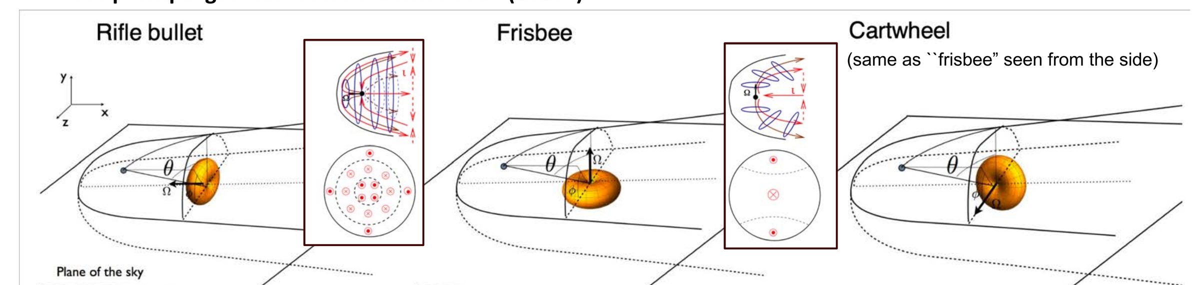

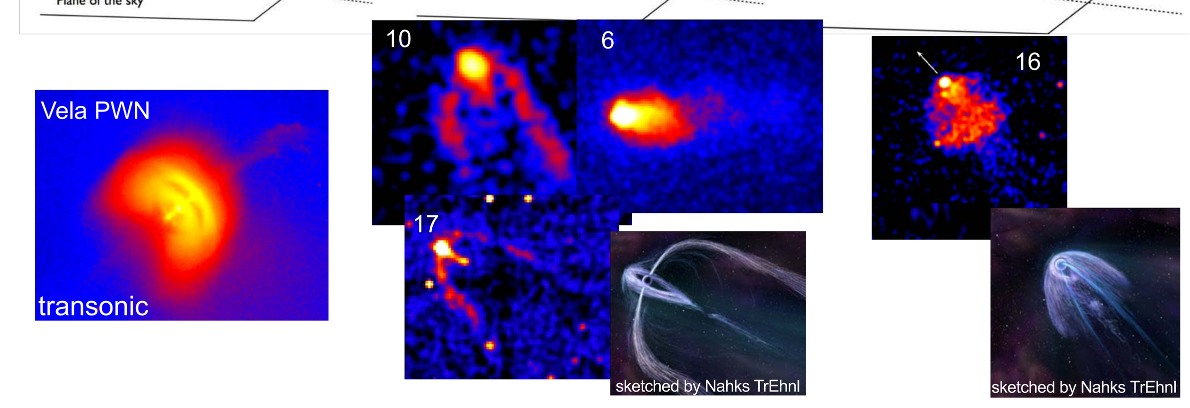

- By linking properties of pulsar gamma-ray and radio light curves and the PWN morphologies one can test the predictions of pulsar magnetosphere models and the SN-kick models.

Long pulsar tails

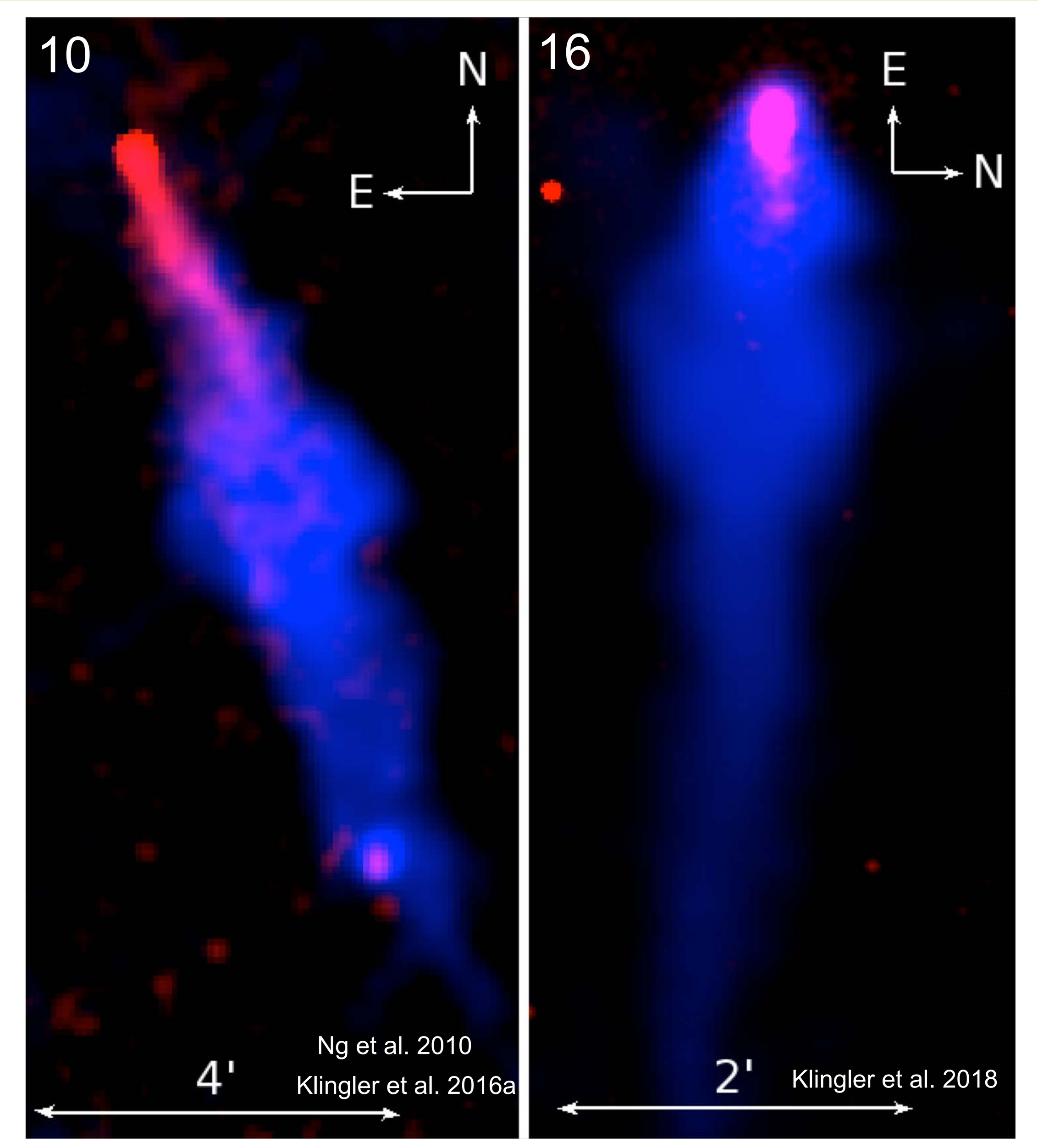

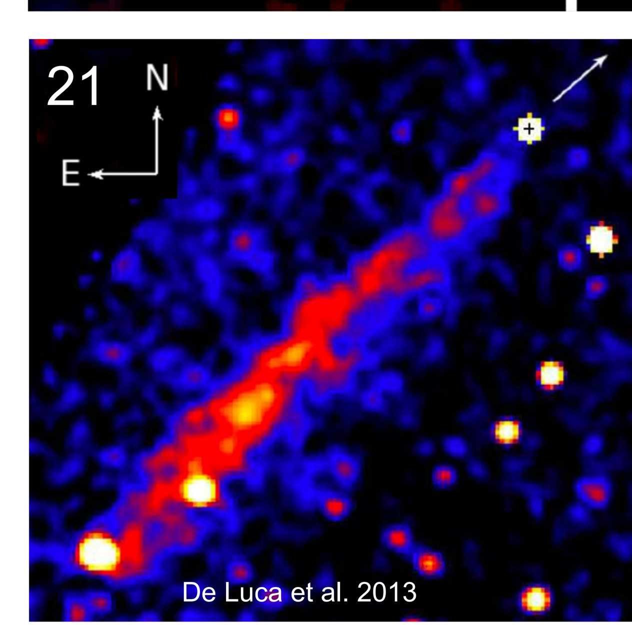

Very different spectral trends for X-ray tails

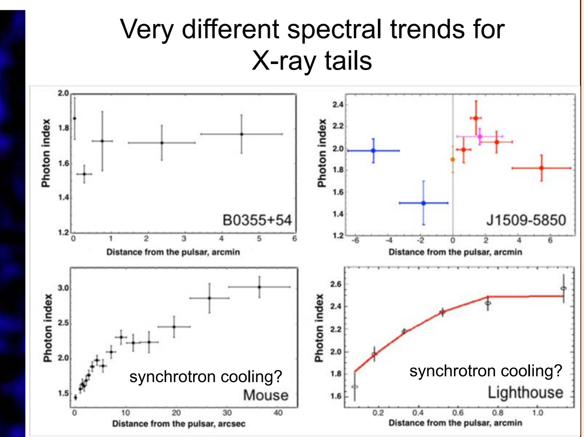

Is this consequence of geometry? The most extended tails show no evidence of softening spectra at large distance from the pulsar. Turbulent heating ? (Xu et al. 2019)

Misaligned outflows (Kinetic jets)

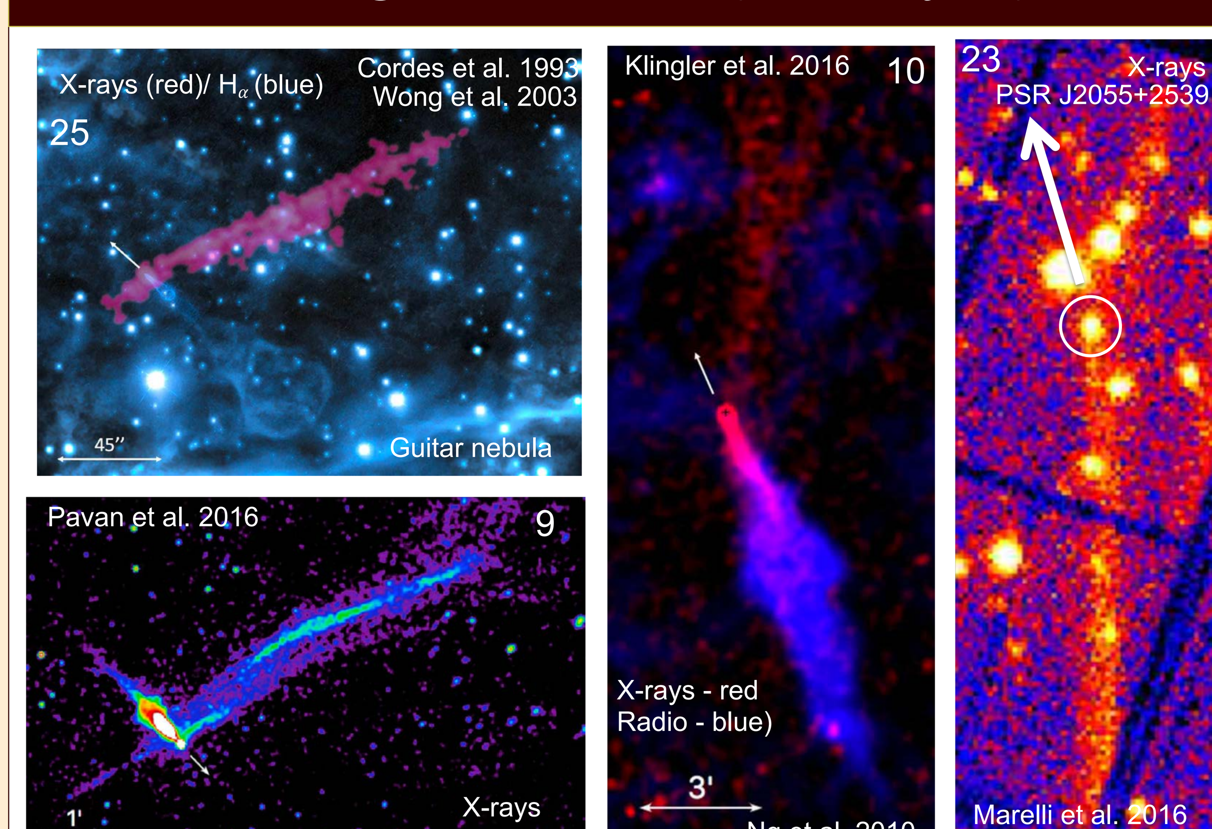

Bandiera (2008): Pulsar wind particles can "leak" kinetically into the surrounding ISM from vicinity of stagnation point if their Larmor radii exceed the standoff distance, R_0.

Bykov et al. (2017): The magnetic field lines in the jets may reconnect with the interstellar magnetic field lines providing a way for the magnetized ultrarelativistic particles to escape into the ISM.

Barkov et al. (2019b): Pulsar wind particles escape into ISM due to reconnection between the PWN and ISM magnetic fields.

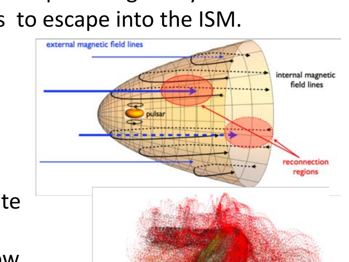

Olmi & Bucciantini (2019b) compute particle trajectories on top of thee 3D MHD model of the flow, and show that not only a beamed escape is possible but that it can be asymmetric and charges can separate.

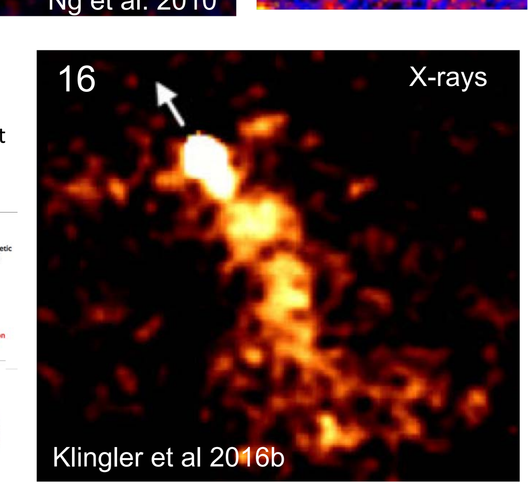

The Guitar nebula, with its well mapped H_α forward shock, is the nearest of these. It offers the best chance to explore the physics of kinetic jets because the pulsar proper motion is very large (175 mas/yr) and accurately measured. The distance (~2 kpc) will be measured accurately from radio parallax. It is an excellent target for a deep study with CXO.

References: ♦ Barkov, M., et al. 2018, MNRAS, 484 4760 ♦ Olmi, B. & Bucciantini, N. 2019a, MNRAS, 484 , 5755 ♦ Olmi, B., et al. 2018, MNRAS, 481, 3394 ♦ Morlino, G., et al. 2015, MNRAS, 454, 3886 ♦ Jankowski, F. et al. 2019, MNRAS, 484, 3691 ♦ Deller, A. et al., 2019, ApJ, 875, 100 ♦ Brownsberger, S. & Romani, R. W. 2014, ApJ, 784, 154 ♦ Rangelov, B. et al., 2017a, ApJ, 835, 264 ♦ Rangelov, B. et al., 2017b, ApJ, 835, 264 ♦ Hui, C. Y. & Becker, W. 2006, A&A, 448, 13 ♦ Stappers B., et al. 2003, Science, 299, 1372 ♦ Kargaltsev, O. et al. 2017, Journal of Plasma Physics, 83, 6301 ♦ Ng, C. -Y., et al. 2012, ApJ, 746, 105 ♦ Tomsick, J., et al. 2012, ApJ, 750, 39 ♦ Ma, Y. K., et al. 2016, ApJ, 820, 100 ♦ Romani, R. W., et al. 2005, ApJ, 631, 480 ♦ Schinzel, F., et al. 2019, ApJ, 876, 17 ♦ Yusef-Zadeh, F. & Gaensler, B. 2005, AdSpR, 35,1129 ♦ Ng, C. -Y., et al., 2010, ApJ, 712, 596 ♦ Klingler, N., et al. 2016a, ApJ, 828, 70 ♦ Klingler et al. 2016b, ApJ, 833, 253 ♦ Klingler, N., et al. 2018, ApJ, 861, 5 ♦ De Luca, A., et al. 2013, ApJ, 765, 19 ♦ Marelli, M., et al. 2016, ApJ, 819, 40 ♦ Cordes, J., et al. 1993, Nature, 362, 133 ♦ Wong, D. S., et al. 2003, IAUS, 214, 135 ♦ Pavan, L., et a. 2016, A&A, 591, 91 ♦ Bandiera, A. 2008, A&A, 490, 3 ♦ Barkov, M., et al. 2019b, MNRAS, 485, 2041 ♦ Bykov, A. M., et al. 2017, Space Science Reviews, 178, 599 ♦ Olmi, B. & Bucciantini, N. 2019b, MNRAS, 490, 3608.